

# Invited Contribution from Recipient of ACS Award for Nuclear Chemistry

## Floating Bands in Nuclear Spectroscopy<sup>†</sup>

Raymond K. Sheline

Chemistry and Physics Departments, Florida State University, Tallahassee, Florida 32306

Received October 8, 1998

The methods of heavy ion nuclear reaction spectroscopy are discussed. When combined with large  $\gamma$  ray arrays and charged particle selection methods, vast amounts of nuclear data are collected and complex nuclear level schemes approaching the extremes of angular momentum result. Often, bands of levels associated with particular nuclei cannot be specifically tied down in the nucleus. Examples of these floating bands are given for  $^{135}\text{Pm}$  and  $^{152}\text{Dy}$ . A correlation of the level schemes of  $^{219}\text{Ra}$ , observed in  $^{223}\text{Th}$   $\alpha$  decay and the nuclear reaction  $^{208}\text{Pb}(^{14}\text{C},3n)$ , suggests that the ground state of  $^{219}\text{Ra}$  has not been observed in the nuclear reaction study. The resultant levels in  $^{219}\text{Ra}$  are then interpreted in terms of a reflection asymmetric nuclear model.

### Introduction

The use of heavy ion reaction spectroscopy with high  $Z$  (atomic number) and  $A$  (mass number) beams has opened a much larger region of the nuclear periodic table and the region of extreme angular momentum to examination. The resulting nuclear level structures are often on the neutron-deficient side because the beams and targets have lower  $N/Z$  ( $N$  = neutron number) than the stable species of the nuclei produced in the reactions.

In addition, there are two other major instrumental developments which have expanded the amount of nuclear data exponentially. The first of these was the large-array Compton suppressed  $\gamma$  detectors such as Gammasphere,<sup>1</sup> which is shown in Figure 1. These large arrays have very high efficiencies, and Compton suppression improves the signal-to-background ratios. Finally, these large arrays make possible triple and higher coincidence studies which further reduce the background. These features allow the study of extremely weak  $\gamma$  transitions and therefore of a much larger volume of total data.

The second important instrumental development was the microball:<sup>2</sup> 95 CsI(Tl) scintillation detectors arranged in an elongated ellipse of revolution and placed inside the large  $\gamma$  array (See Figure 2). The microball detects charged particles ( $^1\text{H}$ ,  $^2\text{H}$ ,  $^3\text{H}$ ,  $^3\text{He}$ , and  $^4\text{He}$ ) and differentiates between them. By demanding coincidences between specific charged particles and the  $\gamma$  ray array, this method turns a potential problem



Raymond K. Sheline was born in Ohio in 1922 and received a B.S. degree in chemistry from Bethany College in West Virginia in 1943. After spending time partly in the military at Columbia University, Oak Ridge, TN, and Los Alamos, NM, on the Manhattan Project, he went to graduate school at Berkeley. Working under K. S. Pitzer, he got his Ph.D. in 1949 studying the molecular spectroscopy of metal complexes. After a two year joint appointment in the Institute for Nuclear Studies and the Chemistry Department at the University of Chicago, he moved to Florida State University in 1951, where he holds the Robert O. Lawton Distinguished Professorship in chemistry and physics. He spent three years on leave from Florida State in 1955–1958 helping to set up a nuclear chemistry laboratory at the Niels Bohr Institute in Copenhagen. His initial research interests were quite broad, spanning the fields of synthesis and spectroscopy of metal complexes and nuclear spectroscopy and structure. In recent years he has concentrated on nuclear studies with primary interest in the spectroscopy and structure resulting from octupole deformation in nuclei. He, in collaboration with his graduate students, postdocs, and colleagues, has generated over 400 publications. His work has been recognized by many awards, the most recent being the American Chemical Society Award for Nuclear Chemistry. He has been a member of the Royal Danish Academy of Sciences since 1974.

<sup>†</sup>This paper is to commemorate scientific achievements of the author, who received the Award for Nuclear Chemistry at the 215th National Meeting of the American Chemical Society, Dallas, TX, March 31, 1998. The text of the Nuclear Chemistry Award Address has been separately published in *J. Phys. Chem.* **1995**, *99*, 7211.

- (1) *GAMMASPHERE, A National Gamma-ray Facility*; Deleplanque, M. A., Diamond, R. M., Eds.; Lawrence Berkeley Laboratory: Berkeley, CA, 1998; PUB-5202. Lee, I. Y. *Nucl. Phys.* **1990**, *A520*, 641c.
- (2) Sarantites, D. G.; Hua, P.-F.; Devlin, M.; Sobotka, L. G.; Elson, J.; Hood, J. T.; LaFosse, D. R.; Sarantites, J. E.; Maier, M. R. *Nucl. Instrum. Methods Phys. Res.* **1996**, *A381*, 418.



**Figure 1.** Gammasphere as set up at Berkeley, showing the Compton suppressed Ge detector systems with the beam pipe coming in from the left. Shown in the figure is project manager Dr. I. Y. Lee, who played an important part in the construction and assembly of Gammasphere. Printed with permission of Prof. Mark Riley, author of "Gammasphere—The Beginning... 1993–1997".

resulting from the numerous reaction channels in a single experiment into a major asset since many of the reaction channels can be separated and studied individually.

As an example of the power of this combination, a single experiment using the  $^{105}\text{Pd}(^{35}\text{Cl},x)$  reaction<sup>3</sup> produced enough data shared among Florida State University, Washington University, The University of Liverpool, and the University of York that five papers and five Ph.D. theses have already resulted, with much more to come.

However, as a result of the exploding volume of nuclear data and semiautomatic methods of analysis, often transitions defining bands, because they are intimately connected with each other by coincidences, are not connected with the rest of the level scheme. These floating bands occur for a variety of reasons. In some cases they end in an isomeric state which cannot be followed further. In other cases there may be large numbers of extremely weak  $\gamma$  transitions, too weak to detect, which depopulate the band.

The heavy ion reactions lead to very high spin states (as will be described in greater detail in the next section). The nucleus then decays through a series of states, ultimately reaching the ground state. However, the floating bands represent relatively high spin states whose exact energies and spins are difficult to

determine since they are not connected with the rest of the level scheme. In some cases the lower spin, low-energy states of a particular nucleus can be studied by other means such as  $\beta$  decay,  $\alpha$  decay, (d,p), (n, $\gamma$ ), etc. These methods often allow the reasonably certain establishment of the energies, spins, and parities of the low-lying part of the level scheme. When there is "cross-talk" between the levels observed in this way and the high-spin bands resulting from heavy ion spectroscopy, it is of great use in tying down the total level scheme. Often, however, the heavy ion reactions lead to such neutron-deficient nuclei that these other methods are not available.

In this paper we will discuss the different methods of studying nuclei with emphasis on the high-spin states, give some typical examples of floating bands, and then give a tentative example of how floating bands can be tied into the rest of the level scheme.

#### Different Experimental Methods. Different Realms of Nuclear Spectroscopy

In this section of the paper we divide the nuclear spectroscopic methods into those which populate the lower energy and lower spin states, and those which populate higher spin states.

Figure 3 is a partial level diagram for  $^{159}\text{Dy}$  showing only the four lower energy configurations (a–d). Also shown in the diagram are the six experimental methods which produced the

(3) Pfohl, J. Dissertation submitted to Florida State University in partial fulfillment of the Ph.D. degree, 1998.



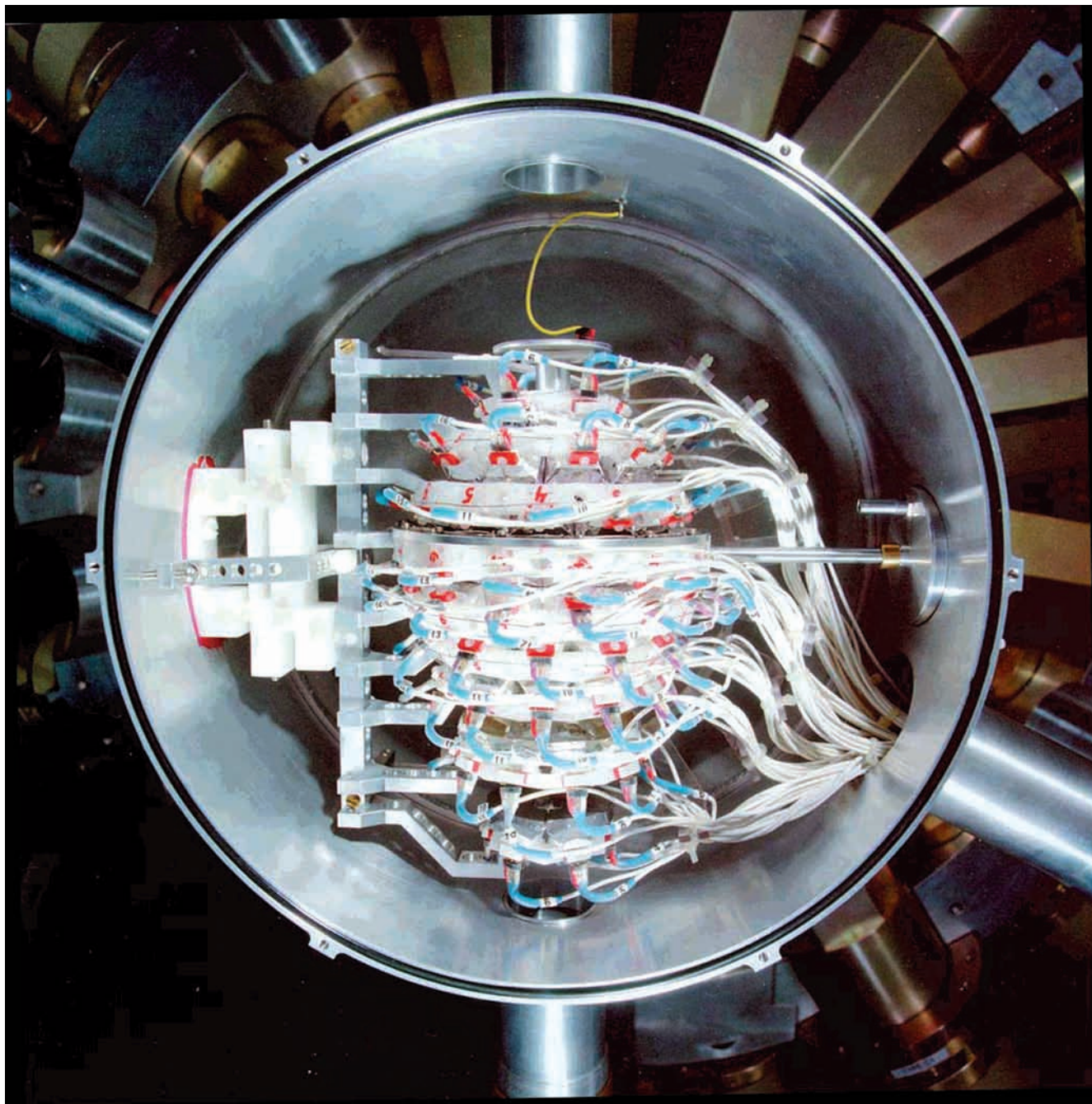


**Figure 2.** The Washington University microball. It consists of 95 CsI(Tl) detector systems and fits neatly inside Gammasphere (Figure 1). It detects the charged particles  ${}^1_2{}^3\text{H}$  and  ${}^3_4\text{He}$  and sorts out reaction channels. Printed with permission of Prof. Mark Riley, author of "Gammasphere—The Beginning... 1993–1997".

level diagram. The level diagram is color coded to show the specific influence of the various experimental methods. For example, the nuclear reactions  ${}^{158}\text{Dy}(d,p){}^{159}\text{Dy}$  and  ${}^{160}\text{Dy}(d,t){}^{159}\text{Dy}$  (A and B),<sup>4</sup> shown in the inset of Figure 3, lead to specific states shown in red which form a superstructure on which the rest of the level scheme can be based. Furthermore, the differential cross sections of the (d,p) and (d,t) reactions and the particle–hole nature of the states resulting from a comparison of the (d,p) and (d,t) cross sections determine the configurations of the bands. Observing the  $\gamma$  rays (shown in green in Figure 3) which result from the electron capture decay of  ${}^{159}\text{Ho}$  and from the isomeric transition of the  $11/2^-$  122  $\mu\text{s}$

state in  ${}^{159}\text{Dy}$  (methods C and D in Figure 3)<sup>5,6</sup> fills in some of the missing states and determines the energies of the states much more accurately. Furthermore, the extremely low log ft (4.81) for electron capture decay of  ${}^{159}\text{Ho}$  to the  $5/2^-$  [523] band head confirms the configuration assignment since the  ${}^{159}\text{Ho}$  ground state with configuration  $7/2^-$  [523] decays by an allowed unhindered transition in which none of the asymptotic quantum numbers within the brackets changes. It should be noted that up through the first four experimental methods (A–D), no spin state higher than  $11/2$  has been populated. However, things change with the last two experimental methods:  ${}^{158}\text{Gd}(\alpha,3n\gamma){}^{159}\text{Dy}$  and  ${}^{160}\text{Gd}(\alpha,5n\gamma){}^{159}\text{Dy}$  (E and F in Figure

(4) Bennett, M. J. Dissertation submitted to Florida State University in partial fulfillment of the Ph.D. degree, 1967.

(5) Boutet, J.; Torres, J. P.; Paris, P. *Nucl. Phys.* **1971**, A167, 326.

(6) Borggreen, J.; Gjaldback, J. P. *Nucl. Phys.* **1968**, A113, 659.

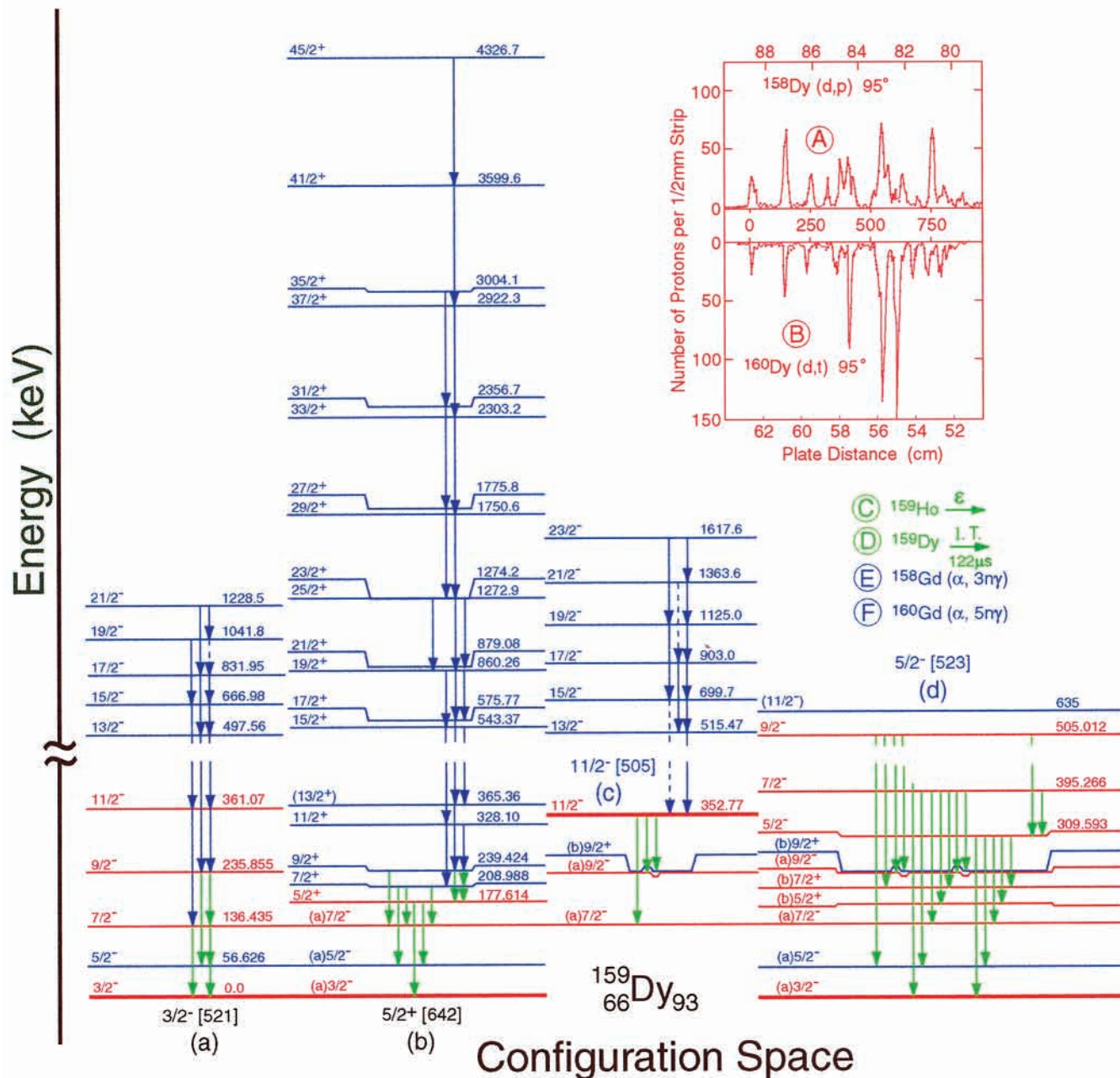


**Figure 3.** Partial level schemes of  $^{159}\text{Dy}$ . The figure is color coded to show what each reaction contributes to the level scheme: red for the charged-particle reactions, green for the electron capture decay of  $^{159}\text{Ho}$  and the isomeric transition of  $^{159}\text{Dy}$ , and blue for the  $(\alpha, xn\gamma)$  reactions.

3, respectively).<sup>7,8</sup> With an  $\alpha$  beam of 60–70 MeV used in reaction F a great deal of angular momentum is brought into the reaction so that states with spins as high as 45/2 can be observed and undoubtedly higher spin states populated but not yet observed. The rationale for these last two methods is presented in the last part of this section. It should be noted here, however, that the transitions shown in blue result only from these last two experimental methods. Fortunately, they connect and coincide with the transitions populating the lower energy and spin states so that the entire level scheme in Figure 3 forms a coherent whole. Therefore we do not have floating bands like those described in the Introduction to this paper. However, in the last part of this section we will describe in detail the methods by which floating bands arise.

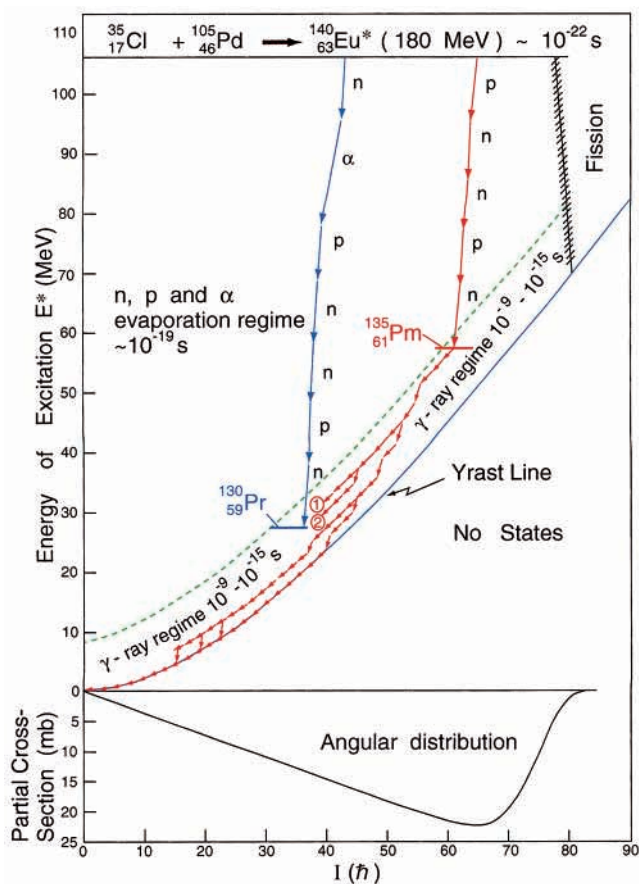
An excellent example of the type of heavy ion reaction which populates high-spin states and may lead to floating bands is a result of a consortium of universities and the Lawrence Berkeley Lab in which Florida State University had the leading role. The reaction was  $^{35}\text{Cl} + ^{105}\text{Pd} \rightarrow ^{140}\text{Eu}^*$ , where  $^{140}\text{Eu}^*$  is a compound nuclear system which then emits neutrons and/or protons and/or  $\alpha$  particles to lead to a wide variety of final nuclei.<sup>3</sup> Thus far 15 different nuclear species have been identified, and there are undoubtedly more. This makes quite clear the importance of the microball, mentioned in the Introduction, for picking out an individual nucleus (or at most a few nuclei) for study.

Figure 4 is a schematic diagram of the processes which occur in this reaction. It is a plot of the energy of excitation  $E^*$  versus the spin  $I$  in units of  $\hbar$ . At the bottom of Figure 4 is plotted the calculated initial angular distribution which is brought into the reaction system. Particularly for chemists, Figure 4 is

(7) Klamra, W.; Hjorth, S. A.; Rensfelt, K. G. *Phys. Scr.* **1973**, 7, 117.

(8) Beuscher, H.; Davidson, W. F.; Lieder, R. M.; Neskakis, A.; Mayer-Borick, C. *Nucl. Phys.* **1975**, A249, 379.





**Figure 4.** Schematic diagram for the nuclear reaction  $^{35}\text{Cl} + ^{105}\text{Pd} \rightarrow ^{140}\text{Eu}^*$  and the processes which follow. At the bottom the calculated angular distribution is shown as a function of cross section. The Yrast line is shown in blue, and neutron or proton binding energies above the Yrast line are shown in green. Particle decay to  $^{135}\text{Pm}$  and  $^{130}\text{Pr}$  is shown schematically in red and blue, respectively. The  $\gamma$  decay is shown only for  $^{135}\text{Pm}$ , and floating bands are labeled 1 and 2.

similar to a phase diagram. At the very top the compound nucleus which lives for only  $\sim 10^{-22}$  s is shown. At the very bottom, the Yrast line is shown in blue. It represents the position of the lowest energy for that particular spin. Therefore no states can exist below this line. Between these two extremes the diagram is divided into two phases which represent regions where different decay modes can occur. With a 180 MeV  $^{35}\text{Cl}$  beam energy, we expect initial spins of the  $^{140}\text{Eu}$  compound system up to  $\sim 80 \hbar$  and an energy of  $\sim 106$  MeV. As long as the nucleus has sufficient energy above the Yrast line (9–10 MeV), the nucleus will emit neutrons, protons, or  $\alpha$  particles in a period of  $\sim 10^{-19}$  s.  $\gamma$  emission is several orders of magnitude slower and cannot compete. However, at energies below the neutron or proton binding energies, the dashed green line in Figure 4,  $\gamma$  emission takes over. Particle emission is shown by near vertical arrows leading from the compound system while  $\gamma$  emission is shown as much shorter arrows, mostly following the Yrast line. For the most part the  $\gamma$  transitions are dipole (E1 or M1) and quadrupole (E2).

Of course a large number of different nuclei are produced in the reaction schematically shown in Figure 4 ( $> 15$ ). We have only indicated two ( $^{135}\text{Pm}$  and  $^{130}\text{Pr}$ ). Furthermore, we have only shown the  $\gamma$  decay for  $^{135}\text{Pm}$  (red in Figure 4) to avoid too much complexity. At the highest spins in the  $\gamma$  ray regime of Figure 4, the level structure may be too complex to disentangle, or it may be cut off by fission. However, as the nucleus cools

it is possible to observe a number of decay pathways, some of which cannot be shown to connect to the Yrast line. These are the floating bands and are given the symbols 1 and 2 in Figure 4. In the next section of this paper we will see directly the level structure of  $^{135}\text{Pr}$  and the bands which are connected to the Yrast line and those which are floating.

### Examples of Floating Bands

In general, floating bands are associated with states connected with the ground state by observing coincidences between the transitions in the floating band and transitions in the band(s) associated with the ground state. However, no explicit transitions connecting the ground state with the floating bands are observed. It is usually assumed that a number of very weak transitions are involved which are below the intensity threshold of the experiment. There are so many floating bands that it is inappropriate to try to give a comprehensive listing. The list is growing quite rapidly with time because the floating bands are being found at a much faster rate than they are being explained away by being connected with the ground state. For that reason, instead of listing floating bands, we give two examples.

**The Floating Bands in  $^{135}\text{Pm}$ .** In Figure 4 we showed schematically the mechanisms by which  $^{135}\text{Pm}$  was produced in the  $^{35}\text{Cl} + ^{105}\text{Pd}$  reaction and its  $\gamma$  decay involving both bands connected with the ground state and floating bands. In Figure 5 we show the actual level scheme of  $^{135}\text{Pm}^3$  in part to indicate the complexity which results with the newest experimental methods and in part to show the presence of floating bands. No attempt is made to consider the complex spectroscopy which involves quite different coexisting nuclear shapes and evolving shape and configuration changes within bands with increasing nuclear spin. These important details will be published elsewhere. Figure 5 is color coded to indicate the floating bands. Floating bands 5, 6, 13, and 14 are shown in red, whereas the rest of the level scheme is shown in blue. The floating bands' exact positions in the level scheme are not known and are shown arbitrarily.

**The Floating Bands in  $^{152}\text{Dy}$ .** The nucleus  $^{152}\text{Dy}$ , with an even number of protons and neutrons, has a special place in the saga of nuclear spectroscopy. It was the first nucleus other than the fission isomers to be shown to have a superdeformed shape in which the 2:1 axis ratio with deformation  $\epsilon = 0.6$  was clearly demonstrated. The nucleus is also interesting because it has moderate oblate deformed states and a normal deformed band.

Figure 5 is a partial level scheme for  $^{152}\text{Dy}^9$  which emphasizes the highly deformed bands observed at high energy. Very often superdeformed bands are floating bands. Figure 6 is color coded with all bands in red corresponding to floating bands. Bands 2–7 are superdeformed, and band 8 is highly deformed but less than superdeformed.

Great effort has been made without success to connect the superdeformed bands in  $^{152}\text{Dy}$  to the ground state. However, this is typical of the mass 150 region. A large number of superdeformed bands are known, and all of them are floating bands.

In the next section we suggest that the entire level structure of  $^{219}\text{Ra}$  observed in a heavy ion reaction is floating, although it has previously been considered to involve the ground state.

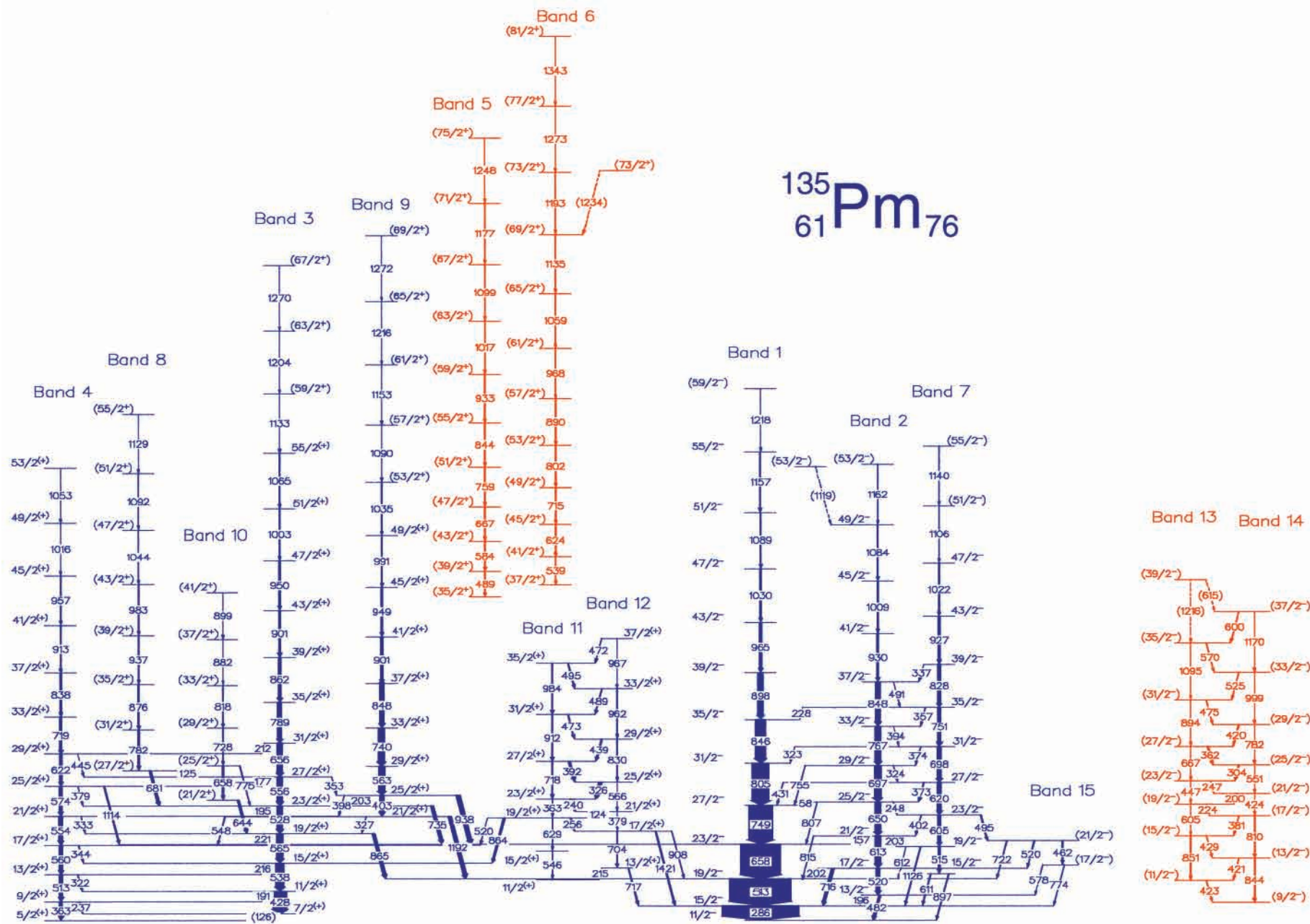


**Figure 5.** Level structure of  $^{135}\text{Pm}$  from the reaction  $^{105}\text{Pd} (^{35}\text{Cl}, 2p3n)$  at 180 MeV. The floating bands are shown in red, and the rest of the level structure is shown in blue.



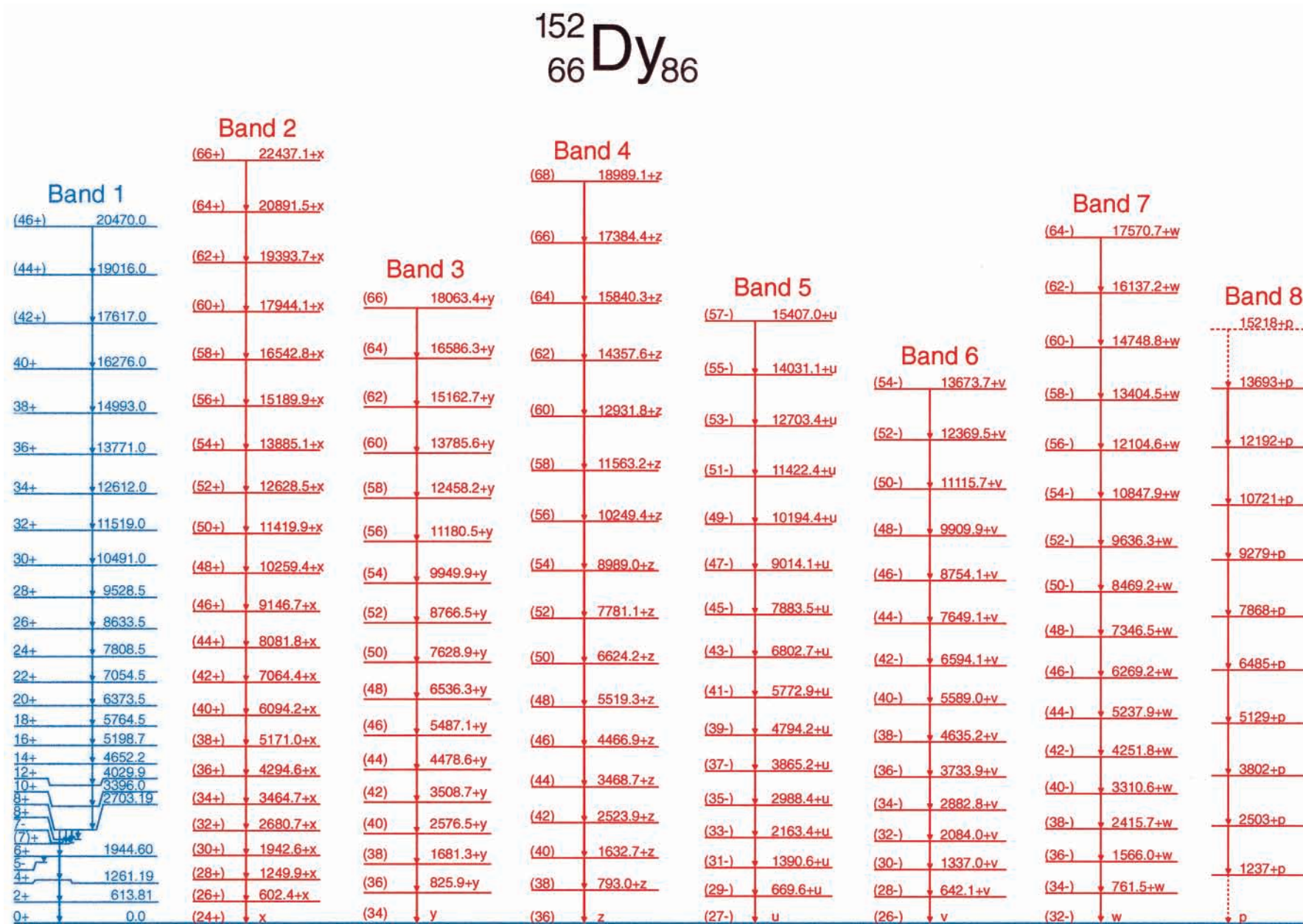
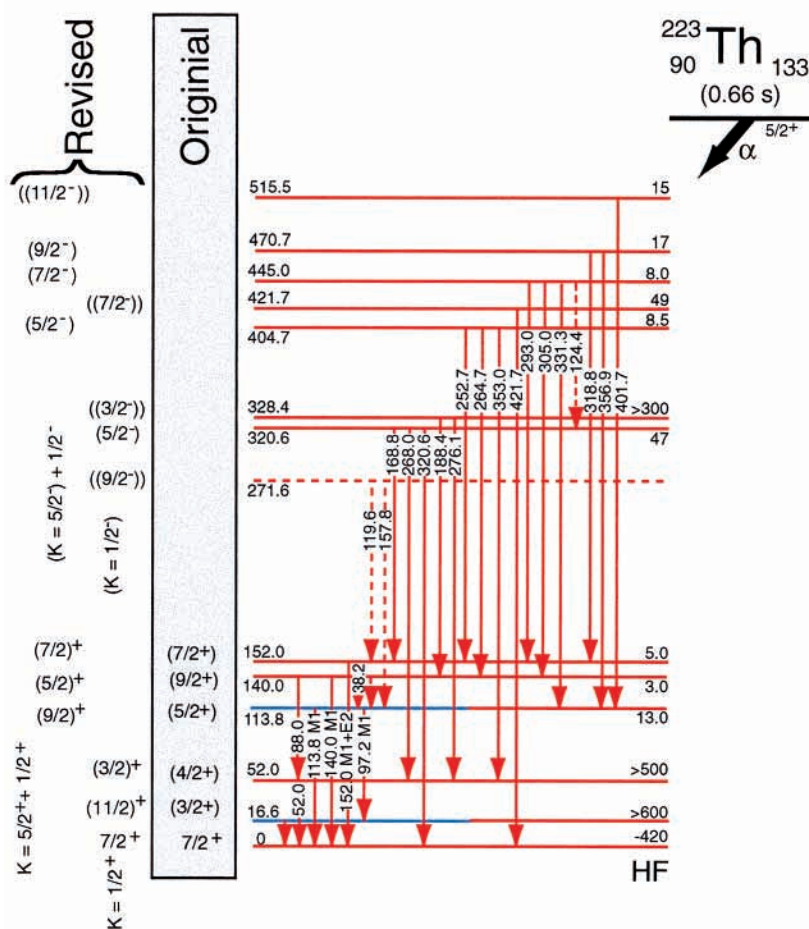


Figure 6. Level structure of  $^{152}\text{Dy}$ . Floating bands are shown in red, and the rest of the level structure is shown in blue.



**Figure 7.** Level scheme of  $^{219}\text{Ra}$  as observed following the  $\alpha$  decay of  $^{223}\text{Th}$ . The spin parities have been revised from those of ref 12 as shown. With this revision the levels shown in half red and half blue correspond to the levels observed in the nuclear reaction study  $^{208}\text{Pb}(^{14}\text{C},3n)$  (Figure 8).

### The Floating Bands in $^{219}\text{Ra}$

In this section we give evidence that the nuclear spectroscopy of  $^{219}\text{Ra}$ , produced in the heavy ion reaction  $^{208}\text{Pb}(^{14}\text{C},3n)^{219}\text{Ra}$ , in reality does not reach the ground state, but represents instead a whole set of floating bands.

The heavy ion reaction spectroscopy<sup>10,11</sup> leads to a quite complex structure, but in both studies extensive band structure is observed. Although the lowest lying band energies in  $^{219}\text{Ra}$  are the same, the assigned spins differ by  $1\hbar$  in the two studies. Alternating spins and opposite parities in this band suggest a weak coupling structure and either static or dynamic reflection asymmetry.

$^{219}\text{Ra}$  has also been studied<sup>12</sup> by observing the  $\alpha$  decay of  $^{223}\text{Th}$ . The  $^{223}\text{Th}$  ground state (with a 0.6 s half-life) has  $J^\pi = 5/2^+$ . Therefore its  $\alpha$  decay is not expected to populate most of the high-spin states observed in the heavy ion reaction studies.<sup>10,11</sup> Even so, as shown in the original assignments in the  $\alpha$  decay study of  $^{223}\text{Th}$  in Figure 7, spins as high as 11/2 have been suggested, which are well within the lower spins proposed

in the heavy ion reaction studies. Therefore one would expect to see some overlap in the spectroscopy between the  $\alpha$  decay and the heavy ion reaction studies. It should also be noted that the extensive regularity observed in the heavy ion reaction studies is completely missing in the  $\alpha$  decay studies.

It can be said without exaggeration that the studies as presented in the literature<sup>10–12</sup> suggest such totally different spectroscopies that we would seem to be dealing with two different nuclei. In consequence, we decided<sup>13</sup> to look more closely at the most recent heavy ion reaction study and the  $\alpha$  decay study to see if we could reconcile the spectroscopies.

**Reconciliation of the Level Structures in  $^{219}\text{Ra}$  Observed in  $\alpha$  Decay and in Heavy Ion Reactions.** We note the presence of a low-lying 97.1 keV transition in ref 11 which is very similar to the 97.2 keV M1 transition observed in the  $\alpha$  decay spectroscopy<sup>12</sup> and Figure 7. However, the original assignment in ref 12 was a  $(5/2^+) \rightarrow (3/2^+)$  transition which would not be populated in the heavy ion spectroscopy. We also note that the 52.0 keV  $(11/2^+) \rightarrow 7/2^+$  transition in the original  $\alpha$  decay spectroscopy should be observed in the heavy ion spectra, but it is not. Both of these anomalies can be corrected by interchanging the  $(11/2^+)$  and  $(3/2^+)$  states at 52.0 and 16.6 keV, respectively, in the  $\alpha$  decay spectra. This in turn requires the interchanging of  $9/2^+$  and  $5/2^+$  states at 140.0 and 113.8 keV, respectively, as shown in Figure 7 revised.

- (10) Cottle, P. C.; Gai, M.; Ennis, J. F.; Shriner, J. F.; Bromley, D. A.; Beausang, C. W.; Hildington, L.; Piel, W. F.; Fossan, D. B.; Olness, J. W.; Warburton, E. K. *Phys. Rev.* **1986**, C33, 1855; **1987**, C36, 2286.  
 (11) Wieland, W.; Niells, J. F.; Reiss, F.; Aiche, M.; Chevallier, A.; Chevallier, J.; Schulz, N.; Sims, J. S.; Briancon, Ch.; Kulesa, R.; Ruchowska, E. *Phys. Rev.* **1992**, C45, 1035.  
 (12) Liang, C. F.; Paris, P.; Gizon, A.; Barci, V.; Barneou, D.; Bernard, R.; Blachot, J.; Briancon, Ch.; Genevey, J.; Sheline, R. K. *Z. Phys.* **1992**, A341, 676.

- (13) Sheline, R. K.; Liang, C. F.; Paris, P. *Czech. J. Phys.* **1993**, 43, 603.



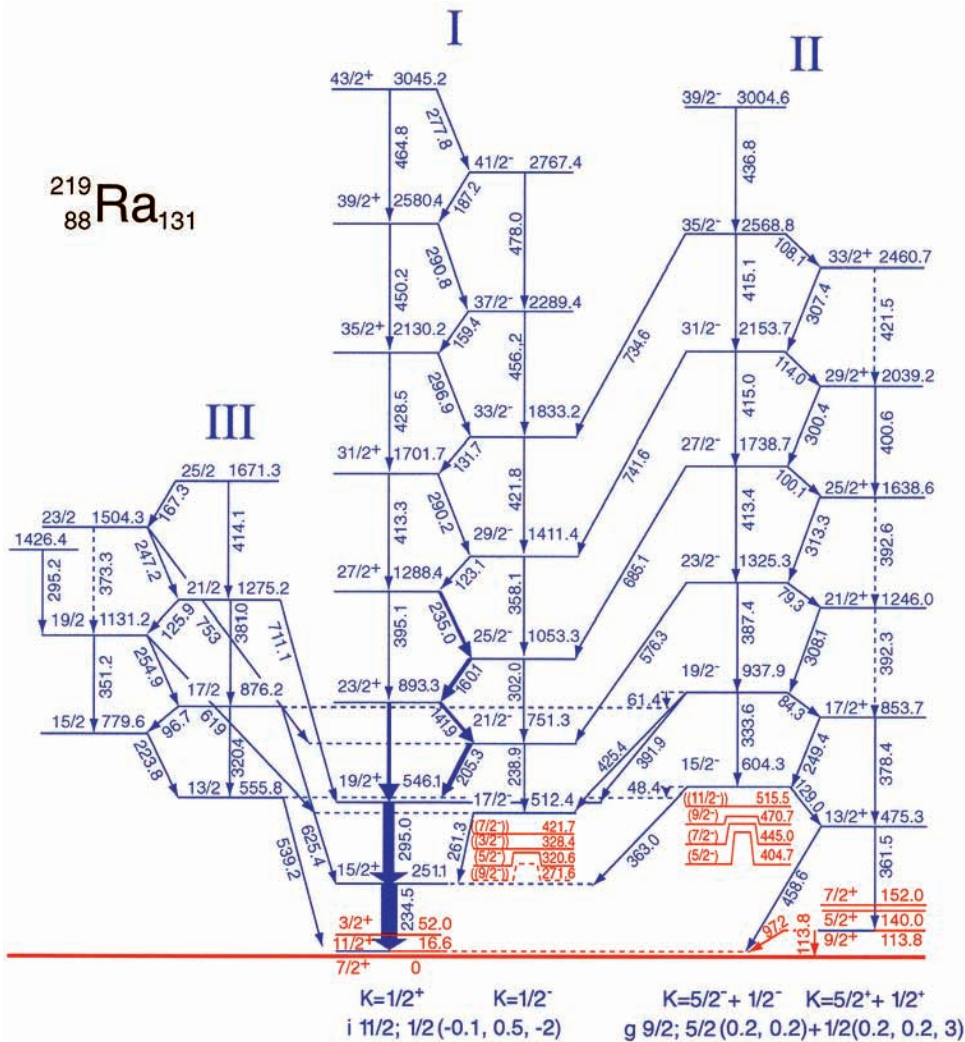


**Figure 8.** Combined level scheme of  $^{219}\text{Ra}$  from the  $\alpha$  decay of  $^{223}\text{Th}$  and the nuclear reaction  $^{208}\text{Pb}(^{14}\text{C},3n)$ . Those levels which are observed in the  $\alpha$  decay are shown in red; those from nuclear reaction spectroscopy are shown in blue; those from both are shown in half red and half blue.  $\gamma$  ray transitions are all from the nuclear reaction study (see Figure 7 for transitions from the  $\alpha$  decay). The 113.8 keV transition is shown in red because of its crucial importance in justifying this level scheme.

Furthermore, the interchange of the  $9/2^+$  and  $5/2^+$  states explains why the hindrance factor (HF) populating the 113.8 keV state is higher than that populating the 140.0 keV state. In addition, the  $7/2^+$ ,  $(11/2^+)$ ,  $(3/2^+)$  revised sequence beginning with the ground state is considered to be a  $K = 1/2^+$  anomalous rotational band as indicated in Figure 7. When the decoupling parameter is calculated for this band, one obtains the value  $-9.03$ , which compares better with the values  $-7.78$  in the isobaric nucleus  $^{219}\text{Fr}^{14}$  than the value  $-5.5$  obtained with the original assignment. In short, no part of the level scheme in Figure 7 is adversely affected by the changes from original to revised. Indeed, the level scheme is improved marginally.

The level scheme of  $^{219}\text{Ra}$  observed in the  $\alpha$  decay of  $^{223}\text{Th}$  is presented in Figure 7. The original spin assignments are shown shaded; the revised assignments also include configurational designations. It should be noted that none of the spin and configurational assignments above 152 keV has been determined experimentally since none of the higher states is connected with lower states by transitions whose multiplicities have been measured. These spins and configura-

tions are suggested by the way the higher states decay and their HFs.

Of course, the main reason for the revision of spin assignments in Figure 7 is to get it to correlate with the heavy ion reaction spectroscopy of ref 11. If we now assume that the  $7/2^+$  ground state of the heavy ion level scheme<sup>11</sup> is in fact the  $11/2^+$  16.6 keV level in the revised  $\alpha$  decay level structure, we are able to reconcile the two level structures with each other. The consequence of this is that all spins of ref 11 would have to be raised by  $2\hbar$  and all energies by 16.6 keV. Thus we see quite clearly that all of the bands in the level schemes of refs 10 and 11 are floating.

The rationale for the failure of the nuclear reaction spectroscopy<sup>10,11</sup> to observe the ground state is quite transparent. The 16.6 keV level should be isomeric with a half-life of  $\approx 10^{-8}$  s. The 16.6 keV E2 transition between the  $(11/2^+)$  first excited state and the  $7/2^+$  ground state would have been missing in the  $\gamma$  ray spectrum of the nuclear reaction spectroscopy because the 16.6 keV state is isomeric and because it is virtually entirely ( $>99.99\%$ ) internally converted. Thus one would have to do an alternative experiment and use an electron detector to see the M, N, etc. electrons which would be difficult in the presence of  $\delta$  rays. The 113.8 keV M1 transition in the  $\alpha$  decay level

(14) Liang, C. F.; Paris, P.; Kvasil, J.; Sheline, R. K. *Phys. Rev.* **1991**, *C44*, 676.

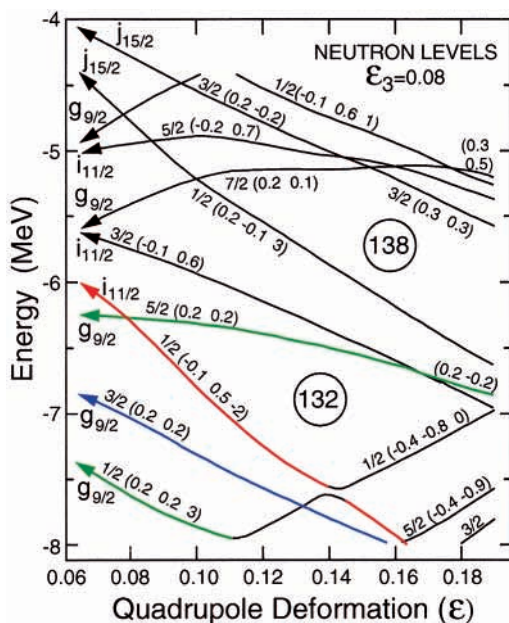


**Figure 9.** Neutron Nilsson levels for finite octupole deformation ( $\epsilon_3 = 0.08$ ). The parity mixed orbitals are labeled by  $\Omega$  ( $\hat{s}_z, \hat{\pi}$ ) and in the case of  $K = 1/2$  orbits a third quantum number ( $\pi \text{ conj} | -\hat{j}_+ | R \text{ conj}$ ). Neutron numbers at gaps are shown in circles. Shell model orbitals at  $\epsilon = \epsilon_3 = 0$  are also given. Orbitals are color coded as described in the text and associated with various bands in Figures 7 and 8.

scheme (Figure 7) which populates the  $^{219}\text{Ra}$  ground state is also observed at 114.0 keV in the nuclear reaction spectroscopy. While it is assigned elsewhere in the level scheme of ref 11, presumably at least a part of this transition fits between the 113.8 keV transition and the ground state. Indeed, it may be necessary to question the upper part of the level scheme<sup>11</sup> where this transition has previously been assigned.

The combined level scheme from  $\alpha$  decay spectroscopy and nuclear reaction spectroscopy is shown in Figure 8. It is color coded to show the levels which come from  $\alpha$  decay spectroscopy (red) and from nuclear reaction spectroscopy (blue). The levels from both kinds of spectroscopy are shown both in red and in blue. The transitions shown all come from the nuclear reaction spectroscopy. The transitions from  $\alpha$  spectroscopy are shown in Figure 7 and are too complex to include in Figure 8. The crucial 113.8 keV transition is, however, shown in red.

**Interpretation of the Level Spectroscopy of  $^{219}\text{Ra}$ .** The nucleus  $^{219}\text{Ra}$  lies on the edge of the region known to involve reflection asymmetric symmetry. For example, its isobar  $^{219}\text{Fr}$  has been interpreted<sup>14</sup> in terms of reflection asymmetry with spectroscopic features such as parity doublet bands (bands close together in energy with the same sets of spins, but opposite parities) and enhanced E1 transitions.

The Nilsson neutron levels plotted against quadrupole deformation for a reflection asymmetric value of  $\epsilon_3 = 0.08$  are shown in Figure 9.<sup>15</sup> If we assume an appropriate quadrupole deformation of 0.09, the 131st neutron of  $^{219}\text{Ra}$  will occupy the  $1/2(-0.1 \ 0.5 \ -2)$  orbital shown in red in Figure 9. This orbital has a large negative decoupling parameter and goes over into the  $i_{11/2}$  shell model state at spherical symmetry. Therefore it provides a natural explanation for the  $7/2^+$ ,  $11/2^+$ ,  $3/2^+$  sequence as members of the  $K = 1/2$  ground-state band labeled I in Figure 8. Furthermore, the negative decoupling parameter suggests why we see the  $15/2^+$ ,  $19/2^+$ ,  $23/2^+$ , ... states instead

of the  $13/2^+$ ,  $17/2^+$ ,  $21/2^+$ , ..., which would require a positive decoupling factor.

In a similar way, we see the very low lying  $K = 5/2^+$  band labeled II in Figure 8 resulting from the  $5/2(0.2 \ 0.2)$  orbital shown in green in Figure 9. It is mixed with the  $1/2(0.2 \ 0.2 \ 3)$  orbital with positive decoupling parameter also shown in green, which explains its anomalous structure and the higher lying sequence  $13/2^+$ ,  $17/2^+$ ,  $21/2^+$ , .... Associated with bands I and II are negative parity bands with opposite simplex, as would be expected for a band system with reflection asymmetry. Finally, there is the band labeled III in Figure 8. Unfortunately, the parities of band members have not been determined, but it may be associated with the  $K = 3/2^+$   $3/2(0.2 \ 0.2)$  orbital shown in blue in Figure 9 also mixed with the  $1/2(0.2 \ 0.2 \ 3)$  orbital mixed with the  $K = 5/2^+$  band.

It should be obvious that a great deal of additional research should be done on  $^{219}\text{Ra}$ . For example, the heavy ion spectroscopy should show a coincidence between the 361.5 keV and the 97.2 and 113.8 keV  $\gamma$  transitions. Experiments are underway at Florida State<sup>16</sup> which show promise in this direction. A search could be undertaken to look for the M, N, ... electrons from the 16.6 keV first excited state. More complete  $\alpha$  spectroscopy to determine spins and parities of all states above 152.0 keV would be very valuable. Finally, the level structure of Figure 8 stands as a challenge to nuclear theorists to see if they can reproduce the evolution of  $K = 1/2$ ,  $3/2$ , and  $5/2$  bands into the level structure actually observed.

## Conclusions

Heavy ion nuclear reaction studies when coupled with the powerful new  $\gamma$  ray spectroscopic methods lead to extremely complex level schemes. Often one observes rotational bands in which sets of transitions are clearly connected to each other and to a particular nucleus, but not discretely to the rest of the level scheme. These floating bands have levels whose exact energies, spins, and parities are therefore unknown. This makes detailed interpretation difficult if not impossible. We have given examples of these floating bands in  $^{135}\text{Pm}$  and  $^{152}\text{Dy}$ . In spite of great effort, it has not been possible to find the connections. Often these floating bands are of the superdeformed type with very large deformation. In the case of  $^{152}\text{Dy}$  these large deformations correspond closely to major to minor axis ratios of 2:1.

Speculation on the reasons why we have not been able to connect the floating bands to the rest of the decay scheme has largely centered on the idea that a large number of different very weak  $\gamma$  rays depopulate the floating bands. Up to now these weak  $\gamma$  rays are below the threshold for observation. Therefore one of the expectations is that even more powerful arrays of  $\gamma$  detectors which will soon come on line may solve some of the floating bands.

A second explanation for floating bands is their possible occurrence when the lowest level in the system is isomeric. This interrupts the coincidence sequence and, unless there is an additional experiment to measure the delayed isomeric transition or a  $\gamma$  ray which bypasses the isomeric level, leaves all the levels above hanging. We propose that this is just the situation which occurs for  $^{219}\text{Ra}$ . By making changes in the level schemes of  $^{219}\text{Ra}$  observed following the  $\alpha$  decay of  $^{223}\text{Th}$  and the nuclear reaction  $^{208}\text{Pb}(^{14}\text{C}, 3n)$  we are able to correlate the two level schemes. The result suggests that the nuclear reaction level scheme was hung up on a 16.6 keV isomeric state so that in

(15) Leander, G. A.; Sheline, R. K. *Nucl. Phys.* **1984**, *A413*, 375.

(16) Riley, L., private communication.



fact all of the levels were floating. This idea is now being tested at the Florida State nuclear facility.

**Acknowledgment.** Support of this study by the State of Florida and the National Science Foundation is gratefully

acknowledged. Jeff Pfohl and Mark Riley made suggestions for the figures, and Lew Riley gave preliminary information on the  $^{219}\text{Ra}$  study at FSU.

IC981196V